

Computational notes on the molecular modeling analyses of flutamide

Mohamed A. M. El-Mansy^{1,2}, Osama Osman³, Abdel Aziz Mahmoud³, Hanan Elhaes⁴, Medhat A. Ibrahim^{3,*}

¹ Molecular Modeling Simulation Lab., Department of Physics, Faculty of Education, Ain Shams University, Roxy, Cairo, Egypt

² Condensed Matter Theory Group, Department of Physics, College of Science and Arts, Qassim University, ArRass, 51921, Saudi Arabia

³ Molecular Spectroscopy and Modeling Unit, Spectroscopy Department, National Research Centre, 33 El-Bohouth St., 12622 Dokki, Giza, Egypt

⁴ Physics Department, Faculty of Women for Arts, Science and Education, Ain Shams University, 11757 Cairo, Egypt

*corresponding author e-mail address: medahmed6@yahoo.com | Scopus ID 8641587100

ABSTRACT

Flutamide is one of the recommended and important drug for treating prostate cancer. In spite of this there some scientific reports that recommending against this drug according to some side effects. This is in turn paves the way towards investigating electronic properties of the drug with conventional molecular modeling methods. So that, density functional theory at B3LYP as well as Hartree-Fock HF together with PM3 were utilized to study the drug. Some important parameters are computed in this computational note including total dipole moment, HOMO/LUMO band gap energy and the contour of molecular electrostatic potential in order to map the active sites of the studied drug in terms the charge distributions. Finally, the infrared assignment of the flutamide is introduced based on B3LYP model.

Keywords: *Flutamide; B3LYP; HF; PM3; Prostate cancer; Electronic properties and Vibrational assignment.*

1. INTRODUCTION

Drug design is one of the recommended fields whereas molecular modeling could be applied [1-2]. Molecular modeling is a class of computer aided computational work to investigate the different properties of molecules in different areas of research and applications [3-7].

Flutamide is an oral, non-steroidal antiandrogen drug primarily used to treat prostate cancer [8-13]. In spite of its well-known application in the treatment of prostate cancer there some reports against it, based on the side effects. Furthermore, the drug is found to be photolabile under UV-B light in either aerobic or anaerobic conditions [14]. Among the adverse impacts, it is stated that liver toxicity including fatal hepatic necrosis is induced as a result of treatment with flutamide [15]. It is also reported that gastrointestinal (GI) was also recorded as a side effect of flutamide during treatment [16]. While it was also reported that, it may induce gynecomastia. In this sense, it is recommended that, the Tamoxifen could partially counteract this effect. Some reports recorded that, patients experience mild liver injury, which resolves when the drug is discontinued. So that, it is recommended in some cases to replace flutamide with bicalutamide as it is recommended for minimization of such side effects [17-18]. This in turn requires scientific efforts in research to overcome these side effects. Accordingly, the drug is supposed to interact with graphdiyne nanotube as nano carrier to enhance its ability to work as anticancer [19]. Another attempt is

to detect flutamide throughout electrochemical detection as the drug with gold electrode [20]. A model serves as a standard tool for flutamide human risk assessment is developed. This model was developed for the harmonized whole body physiologically based pharmacokinetic or flutamide in rats the further extrapolated to humans [21]. The residue of the drug in urine with a topic of research interest. So that, the electrochemical behavior of flutamide is further studied with carbon paste electrode modified by CuO/GO/PANI nanocomposite [22]. Spectroscopic determination of the residue of the drug in the environmental samples paves the way to researchers to develop analytical methods for determinations of flutamide. lanthanum cobaltite decorated halloysite nanotube (LCO/HNT) nanocomposite was used for the fast and direct determination of flutamide in environmental samples [23]. Some physical parameters are calculated with molecular modeling show the ability to describe the reactivity of a given molecular system. These parameters including total dipole moment, HOMO/LUMO band gap energy and molecular electrostatic potential [24-29]. In this sense molecular modeling is dedicated to studying flutamide to indicate its reactivity in terms total dipole moment and band gap energy while the active sites are indicated while the molecular electrostatic potential is mapped. Therefore, the present computational notes are conducted.

2. MATERIALS AND METHODS

Calculation Details.

A model molecule for flutamide was built as indicated in figure 1. Model molecule was calculated with G09 program system [30] at Spectroscopy Department, National Research Centre. The optimization was performed at three levels including PM3, HF/6-

31gd,p) and DFT: B3LYP/6-31g(d,p) [31-33]. Total dipole moment, HOMO/LUMO band gap energy and Molecular electrostatic potential are calculated. Vibrational calculations and assignment was conducted at B3LYP/6-31g(d,p).

3. RESULTS

Figure 1 presents the model structure of the studied flutamide which is subjected to optimization at B3LYP/6-31g(d,p), HF/6-31g(d,p) and PM3 levels. To describe the reactivity of the flutamide, the band gap energy is calculated as the difference between highest occupied molecular orbit and lowest unoccupied molecular orbit HOMO/LUMO. Figure 2 presents the mapping of both HOMO/LUMO whereas the band gap at B3LYP/6-31g(d,p) was 4.486 eV while the total dipole moment was 8.815 Debye.

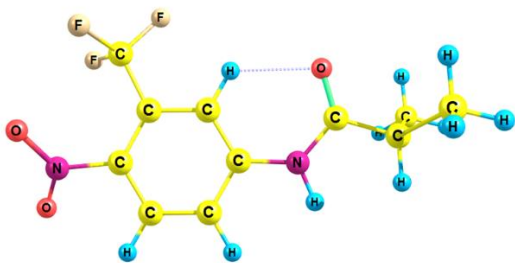


Figure 1. Model structure of the studied Flutamide.

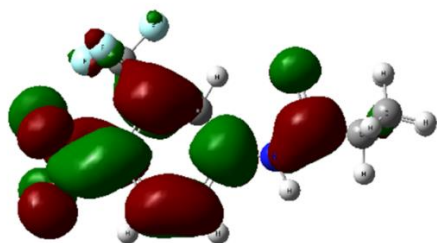


Figure 2. Calculated B3LYP/6-31g(d,p) HOMO/LUMO band gap energy as 4.486 eV while the total dipole moment is 8.815 Debye.

Another description for reactivity could be described as in figure 3 for the contour of molecular electrostatic potential MESP.

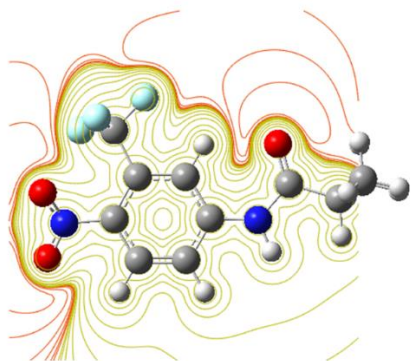


Figure 3. Mapping the contours of molecular electrostatic potential which is calculated at B3LYP/6-31g(d,p).

Correlation between reactivity and charge distribution is previously reported. The distribution of charge is given by contours with different colors [34-36]. It is stated that MESP is following the color scheme according to the following increasing orders: red < orange < yellow < green < blue. Blue indicates the highest MESP, while red indicates the lowest MESP.

Regarding the contour of MESP in figure 3 it is clear that active sites are surrounding oxygen and fluorine atoms which indicated that nearly all the sites in the studied molecules are reactive.

2.1. Vibrational Assignments.

For the studied optimized structure another important parameter could be also calculated namely the vibrational spectra calculations.

Besides its importance in the assignment of the given structure as computational methods providing the facility of the assignment of the calculated spectra. This calculation is another confirmation for the optimization of the studied structure as one obtain small frequencies tend to zero and/or positive frequencies rather than negative frequencies which indication for transition states not optimized structures.

Three level of theories were followed for the calculation of the IR spectrum of flutamide.

Title molecule has 84 (67 actives & 17 in actives) probable vibrational modes. Only 19 modes with remarkable intensities have been chosen (16 A' + 3 A''). The computed wavenumbers and the corresponding assignments at B3LYP/6-31G(d,p), HF/6-31G(d,p) and PM3 ZDO are presented in Table 1. The calculated IR charts at B3LYP/6-31G(d,p), HF/6-31G(d,p) and PM3 ZDO are presented in Figures 4, 5 and 6 respectively. Assignments are based upon computationally predicted wavenumbers visualized by GV5 program. Predicted assignments at B3LYP/6-31G(d,p) have been discussed briefly as in the following

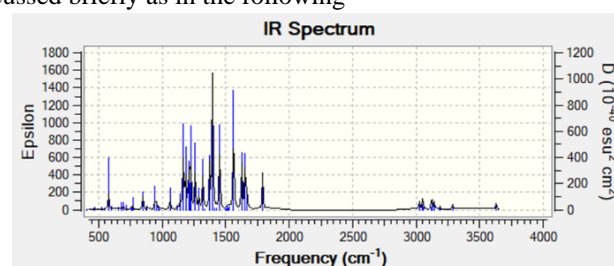


Figure 4. IR spectrum for flutamide which is calculated at B3LYP/6-31g(d,p) level.

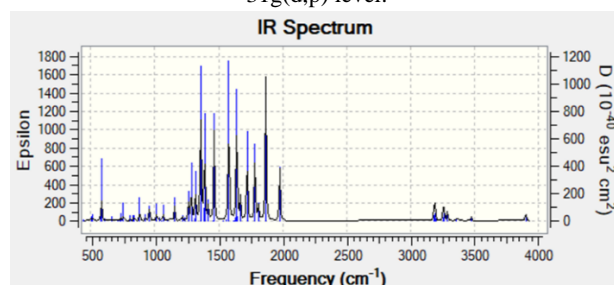


Figure 5. IR spectrum for flutamide which is calculated at HF/6-31g(d,p) level.

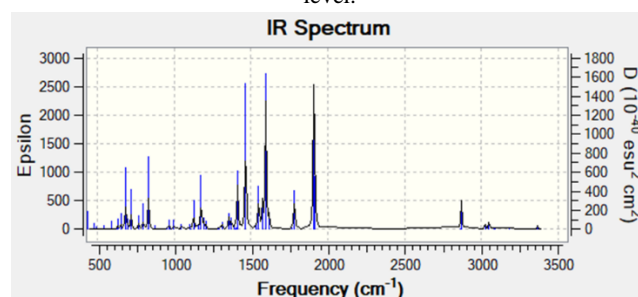


Figure 6. IR spectrum for flutamide which is calculated at semiempirical PM3 level.

2.2. Single bond vibrations.

Mode (19,18) are recognized respectively to N-H and C-H stretch at 3621 and 3287 cm^{-1} at B3LYP/6-31G(d,p). Modes (17,16) are specified for both symmetric and asymmetric C-H stretch at 3123, 3024 cm^{-1} . Modes (10,9) are assigned to N-H bend-in at 1398, 1321 cm^{-1} while modes (8-6) are attributed to C-H bend-in at 1260, 1185 and 1166 cm^{-1} , respectively. Mode (3,4) are

referred to both N-H and C-H bend-out at 851 and 768 cm^{-1} , respectively.

Mode (11) is attributed as CH_3 deformations at 1553 cm^{-1} at B3LYP/6-31G(d,p). Mode (1) is specified for C-F + C-N + C-C bend-in at 578 cm^{-1} . While modes (5,4) are assigned to C-F+C-N and C-C stretch at 1064 and 953 cm^{-1} , respectively.

2.3. Double bond vibrations.

C=O, C=C stretch are noticed at range 1750-1560 cm^{-1} . Modes (15,14) are specified to C=O stretch at 1791 and 1668 cm^{-1} , respectively. Modes (13,12) are recognized to C=C stretch at 1654 and 1562 cm^{-1} , respectively.

Table 1. Calculated IR spectrum for flutamide and their band assignment which calculated at three levels namely B3LYP/6-31G(d,p), HF/6-31G(d,p) and PM3 semiempirical level.

| No | B3LYP/6-31G(d,p) | | HF/6-31G(d,p) | | PM3 | | Vibrational Assignments |
|----|---------------------------------|--------------|---------------------------------|--------------|---------------------------------|--------------|---|
| | Wavenumber (cm^{-1}) | IR Intensity | Wavenumber (cm^{-1}) | IR Intensity | Wavenumber (cm^{-1}) | IR Intensity | |
| 1 | 578 | 58 | 586 | 67 | 684 | 111 | β C-F + β C-N + β C-C |
| 2 | 768 | 17 | 754 | 25 | 720 | 75 | γ C-H |
| 3 | 851 | 24 | 881 | 38 | 833 | 160 | γ N-H |
| 4 | 953 | 8 | 960 | 26 | 971 | 22 | ν C-C |
| 5 | 1064 | 43 | 1065 | 32 | 1047 | 13 | ν C-F + ν C-N |
| 6 | 1166 | 191 | 1155 | 19 | 1127 | 85 | β C-H |
| 7 | 1185 | 143 | 1263 | 68 | 1176 | 168 | |
| 8 | 1260 | 162 | 1285 | 137 | 1192 | 36 | |
| 9 | 1321 | 128 | 1358 | 386 | 1373 | 42 | β N-H |
| 10 | 1398 | 159 | 1389 | 274 | 1413 | 218 | |
| 11 | 1553 | 237 | 1464 | 287 | 1465 | 562 | CH_3 deformations |
| 12 | 1562 | 358 | 1578 | 462 | 1550 | 175 | ν C=C |
| 13 | 1654 | 179 | 1641 | 395 | 1596 | 655 | |
| 14 | 1668 | 68 | 1669 | 74 | 1789 | 183 | ν C=O |
| 15 | 1791 | 128 | 1721 | 282 | 1909 | 674 | |
| 16 | 3024 | 33 | 3183 | 47 | 2869 | 145 | ν_s C-H |
| 17 | 3123 | 39 | 3189 | 43 | 3023 | 29 | ν_{as} C-H |
| 18 | 3287 | 22 | 3258 | 61 | 3084 | 45 | ν C-H |
| 19 | 3629 | 24 | 3900 | 40 | 3364 | 17 | ν N-H |

ν (stretch); ν_s (symmetric-stretch); ν_{as} (asymmetric-stretch); β (bend-in); γ (bend-out)

4. CONCLUSIONS

Molecular modeling at DFT, HF and semiempirical methods show the ability to study the reactivity and vibrational spectra of drugs such as flutamide.

For such a small molecule it is indicated that the studied models show comparable results. The present computational

models could be useful to draw the reactivity and lead the research for controlling drugs in terms of their reactivity which in turn could suggest a solution in term substations of active sites or minimizing the adverse impacts if it exists.

5. REFERENCES

- Ibrahim, M.; Saleh, N.A.; Elshemey, W.M.; Elsayed, A.A. Hexapeptide functionality of cellulose as NS3 protease inhibitors. *Med Chem* **2012**, *8*, 826-830, <https://doi.org/10.2174/157340612802084144>.
- Ibrahim, M.; Saleh, N.A.; Elshemey, W.M.; Elsayed, A.A. Fullerene derivative as anti-HIV protease inhibitor: molecular modeling and QSAR approaches. *Mini Rev Med Chem* **2012**, *12*, 447-451, <https://doi.org/10.2174/138955712800493762>.
- Nashy, E.H.A.; Osman, O.; Mahmoud, A.A.; Ibrahim, M. Molecular spectroscopic study for suggested mechanism of chrome tanned leather. *Spectrochimica Acta Part A: Molecular and Biomolecular Spectroscopy* **2012**, *88*, 171-176, <https://doi.org/10.1016/j.saa.2011.12.024>.
- Ibrahim, M.; El-Barbary, A.A.; El-Nahass, M.M.; Kamel, M.A.; El-Mansy, M.A.M.; Asiri, A.M. On the spectroscopic analyses of (E)-3-(dicyclopropyl methylene)-dihydro-4-[1-(2,5 dimethylfuran-3-yl) ethylidene]furan-2,5-dione. *Spectrochimica Acta Part A: Molecular and Biomolecular Spectroscopy* **2012**, *87*, 202-208, <https://doi.org/10.1016/j.saa.2011.11.039>.
- Badry, R.; Omar, A.; Mohammed, H.; Mohamed, D.A.A.; Elhaes, H.; Refaat, A.; Ibrahim, M. Effect of Alkaline Elements on the Structure and Electronic properties of Glycine. *Biointerface Research in Applied Chemistry* **2018**, *8*, 3682-3687.
- Badry, R.; Ghanem, A.S.A.E.; Ahmed, H.; Fahmy, A.; Elhaes, H.; Refaat, A.; Ibrahim, M. Effect of Li, Na, K, Be, Mg and Ca on the electronic properties, geometrical parameters of carboxylic acids. *Biointerface Research in Applied Chemistry* **2018**, *8*, 3657-3660.
- Bayoumy, A.M.; Badry, R.; Gaber, H.A.; Elbiomy, S.A.; El Gabaly, S.G.; Abd ElAziz, M.S.; Gouda, S.M.; Elhaes, H.; Yahia, I.S.; Zahran, H.Y.; Ibrahim, M. Molecular modeling analyses for the effect of solvents on amino acids. *Biointerface Research in Applied Chemistry* **2019**, *9*, 4379-4383.
- Small, E.J. Prostate cancer. *Current Opinion in Oncology* **1997**, *9*, 277-286, <https://doi.org/10.1097/00001622-199709030-00011>.
- Dacker, R. Chemotherapy and prostate cancer. *Radiol. Technol.* **1997**, *68*, 194-195.
- Ornstein, D.K.; Rao, G.S.; Johnson, B.; Charlton, E.T.; Andriole, G.L. Combined finasteride and flutamide therapy in men with advanced prostate cancer. *Urology* **1996**, *48*, 901-905, [https://doi.org/10.1016/S0090-4295\(96\)00315-9](https://doi.org/10.1016/S0090-4295(96)00315-9).
- Boccon-Gibod, L.; Fournier, G.; Bottet, P.; Marechal, J.M.; Guiter, J.; Rischman, P.; Hubert, J.; Soret, J.Y.; Mangin, P.; Mallo, C.; Frayssse, C.E. Flutamide versus orchidectomy in the treatment of metastatic prostate carcinoma. *Eur Urol* **1997**, *32*, 391-395.

12. Mahler, C.; Verhelst, J.; Denis, L. Clinical Pharmacokinetics of the Antiandrogens and Their Efficacy in Prostate Cancer. *Clinical Pharmacokinetics* **1998**, *34*, 405-417, <https://doi.org/10.2165/00003088-199834050-00005>.
13. Vargas, F.; Rivas, C.; Méndez, H.; Fuentes, A.; Fraile, G.; Velásquez, M. Photochemistry and phototoxicity studies of flutamide, a phototoxic anti-cancer drug. *Journal of Photochemistry and Photobiology B: Biology* **2000**, *58*, 108-114, [https://doi.org/10.1016/s1011-1344\(00\)00110-x](https://doi.org/10.1016/s1011-1344(00)00110-x).
14. Kashimshetty, R.; Desai, V.G.; Kale, V.M.; Lee, T.; Moland, C.L.; Branham, W.S.; New, L.S.; Chan, E.C.Y.; Younis, H.; Boelsterli, U.A. Underlying mitochondrial dysfunction triggers flutamide-induced oxidative liver injury in a mouse model of idiosyncratic drug toxicity. *Toxicology and Applied Pharmacology* **2009**, *238*, 150-159, <https://doi.org/10.1016/j.taap.2009.05.007>.
15. Crownover, R.L.; Holland, J.; Chen, A.; Krieg, R.; Young, B.K.; Roach, M., III; Fu, K.K. Flutamide-induced liver toxicity including fatal hepatic necrosis. *International Journal of Radiation Oncology • Biology • Physics* **1996**, *34*, 911-915, [https://doi.org/10.1016/0360-3016\(95\)02107-8](https://doi.org/10.1016/0360-3016(95)02107-8).
16. Langenstroer, P.; Porter, H.J.; Mc, L.D.G.; Thrasher J, B. Direct Gastrointestinal Toxicity of Flutamide: Comparison of Irradiated and Nonirradiated Cases. *Journal of Urology* **2004**, *171*, 684-686, <https://doi.org/10.1097/01.ju.0000106835.60202.81>.
17. Martinović-Weigelt, D.; Wang, R.-L.; Villeneuve, D.L.; Bencic, D.C.; Lazorchak, J.; Ankley, G.T. Gene expression profiling of the androgen receptor antagonists flutamide and vinclozolin in zebrafish (*Danio rerio*) gonads. *Aquatic Toxicology* **2011**, *101*, 447-458, <https://doi.org/10.1016/j.aquatox.2010.10.003>.
18. Rajakumar, A.; Singh, R.; Chakrabarty, S.; Muruganankumar, R.; Laldinsangi, C.; Prathibha, Y.; Sudhakumari, C.C.; Dutta-Gupta, A.; Senthikumar, B. Endosulfan and flutamide impair testicular development in the juvenile Asian catfish, *Clarias batrachus*. *Aquatic Toxicology* **2012**, *110-111*, 123-132, <https://doi.org/10.1016/j.aquatox.2011.12.018>.
19. Nagarajan, V.; Chandiramouli, R. Flutamide drug interaction studies on graphdiyne nanotube – A first-principles study. *Computational and Theoretical Chemistry* **2019**, *1167*, <https://doi.org/10.1016/j.comptc.2019.112590>.
20. Mehrabi, A.; Rahimnejad, M.; Mohammadi, M.; Pourali, M. Electrochemical detection of flutamide with gold electrode as an anticancer drug. *Biocatalysis and Agricultural Biotechnology* **2019**, *22*, <https://doi.org/10.1016/j.bcab.2019.101375>.
21. Sharma, R.P.; Kumar, V.; Schuhmacher, M.; Kolodkin, A.; Westerhoff, H.V. Development and evaluation of a harmonized whole body physiologically based pharmacokinetic (PBPK) model for flutamide in rats and its extrapolation to humans. *Environmental Research* **2020**, *182*, <https://doi.org/10.1016/j.envres.2019.108948>.
22. Afzali, M.; Mostafavi, A.; Shamspur, T. Square wave voltammetric determination of anticancer drug flutamide using carbon paste electrode modified by CuO/GO/PANI nanocomposite. *Arabian Journal of Chemistry* **2020**, *13*, 3255-3265, <https://doi.org/10.1016/j.arabjc.2018.11.001>.
23. Suvina, V.; Kokulnathan, T.; Wang, T.J.; Balakrishna, R.G. Unraveling the electrochemical properties of lanthanum cobaltite decorated halloysite nanotube nanocomposite: An advanced electrocatalyst for determination of flutamide in environmental samples. *Ecotoxicology and Environmental Safety* **2020**, *190*, <https://doi.org/10.1016/j.ecoenv.2019.110098>.
24. Ezzat, H.A.; Hegazy, M.A.; Nada, N.A.; Ibrahim, M.A. Effect of Nano Metal Oxides on the Electronic Properties of Cellulose, Chitosan and Sodium Alginate. *Biointerface Research in Applied* **2019**, *9*, 4143-4149.
25. Ibrahim, M.; El-Haes, H. Computational Spectroscopic Study of Copper, Cadmium, Lead and Zinc Interactions in the Environment. *Int. J. Environ. Pollut.* **2005**, *23*, 417-424, <http://dx.doi.org/10.1504/IJEP.2005.007604>.
26. Ibrahim, M.; Mahmoud, A.A. Computational Notes on the Reactivity of Some Functional Groups. *Journal of Computational and Theoretical Nanoscience* **2009**, *6*, 1523-1526, <https://doi.org/10.1166/jctn.2009.1205>.
27. Abdelsalam, H.; Saroka, V.A.; Ali, M.; Teleb, N.H.; Elhaes, H.; Ibrahim, M.A. Stability and electronic properties of edge functionalized silicene quantum dots: A first principles study. *Physica E: Low-dimensional Systems and Nanostructures* **2019**, *108*, 339-346, <https://doi.org/10.1016/j.physe.2018.07.022>.
28. Grenni, P.; Barra Caracciolo, A.; Mariani, L.; Cardoni, M.; Riccucci, C.; Elhaes, H.; Ibrahim, M.A. Effectiveness of a new green technology for metal removal from contaminated water. *Microchemical Journal* **2019**, *147*, 1010-1020, <https://doi.org/10.1016/j.microc.2019.04.026>.
29. Arteca, G.A.; Jammal, V.B.; Mezey, P.G.; Yadav, J.S.; Hermsmeier, M.A.; Gund, T.M. Shape group studies of molecular similarity: relative shapes of Van der Waals and electrostatic potential surfaces of nicotinic agonists. *Journal of Molecular Graphics* **1988**, *6*, 45-53, [https://doi.org/10.1016/0263-7855\(88\)80061-4](https://doi.org/10.1016/0263-7855(88)80061-4).
30. Frisch, M.J.; Trucks, G.W.; Schlegel, H.B.; Scuseria, G.E.; Robb, M.A.; Cheeseman, J.R.; Scalmani, G.; Barone, V.; Mennucci, B.; Petersson, G.A. Gaussian09, revisions D. 01 and B. 01; Gaussian, Inc. Wallingford, CT **2010**.
31. Becke, A.D. Density-functional thermochemistry. III. The role of exact exchange. *J. Chem. Phys.* **1993**, *98*, 5648-5652, <https://doi.org/10.1063/1.464913>.
32. Lee, C.; Yang, W.; Parr, R.G. Development of the Colle-Salvetti correlation-energy formula into a functional of the electron density. *Physical Review B* **1988**, *37*, 785-789, <https://doi.org/10.1103/PhysRevB.37.785>.
33. Miehlich, B.; Savin, A.; Stoll, H.; Preuss, H. Results obtained with the correlation energy density functionals of Becke and Lee, Yang and Parr. *Chemical Physics Letters* **1989**, *157*, 200-206, [https://doi.org/10.1016/0009-2614\(89\)87234-3](https://doi.org/10.1016/0009-2614(89)87234-3).
34. Politzer, P.; Laurence, P.R.; Jayasuriya, K. Molecular electrostatic potentials: an effective tool for the elucidation of biochemical phenomena. *Environmental Health Perspectives* **1985**, *61*, 191-202, <https://doi.org/10.1289/ehp.8561191>.
35. Politzer, P.; Murray, J.S. Relationships of Electrostatic Potentials to Intrinsic Molecular Properties. In: *Theoretical and Computational Chemistry*, Murray, J.S.; Sen, K. Eds. Elsevier: Volume 3, 1996; pp. 649-660, [https://doi.org/10.1016/S1380-7323\(96\)80056-2](https://doi.org/10.1016/S1380-7323(96)80056-2).
36. Şahin, Z.S.; Şenöz, H.; Tezcan, H.; Büyükgüngör, O. Synthesis, spectral analysis, structural elucidation and quantum chemical studies of (E)-methyl-4-[(2-phenylhydrazono)methyl]benzoate. *Spectrochimica Acta Part A: Molecular and Biomolecular Spectroscopy* **2015**, *143*, 91-100, <https://doi.org/10.1016/j.saa.2015.02.032>.

